Dalton Transactions

PAPER

View Article Online
View Journal | View Issue

Cite this: *Dalton Trans.*, 2017, **46**, 9824

Chalcogenoether complexes of Nb(v) thio- and seleno-halides as single source precursors for low pressure chemical vapour deposition of NbS_2 and $NbSe_2$ thin films†

Yao-Pang Chang, Andrew L. Hector, William Levason and Gillian Reid *

$NbSCl_3$ was obtained *via* reaction of $NbCl_5$ with $S(SiMe_3)_2$ in anhydrous CH_2Cl_2, whilst in MeCN solution the same reaction gives $[NbSCl_3(MeCN)_2]$. $[NbSeCl_3(MeCN)_2]$ was obtained similarly from $NbCl_5$ with $Se(SiMe_3)_2$. The chalcogenoether complexes, $[NbSCl_3(ER_2)]$ (E = S: R = Me, ^{n}Bu; E = Se: R = ^{n}Bu), were obtained from reaction of $NbCl_5$, ER_2 and $S(SiMe_3)_2$ in CH_2Cl_2. The structure of the $[Nb_2S_2Cl_6(SMe_2)_2]$ reveals a Cl-bridged dimer with the SMe_2 ligands disposed *syn*. The Cl bridges are highly asymmetric, with the long Nb–Cl bond *trans* Nb=S. The complexes, $[NbSCl_3(L–L)]$ (L–L = $MeSCH_2CH_2SMe$, $MeS(CH_2)_3SMe$, ^{i}PrSCH$_2$CH$_2$S^{i}Pr, $MeSe(CH_2)_3SeMe$ and ^{n}BuS$(CH_2)_3$S^{n}Bu), were obtained from reaction of L–L with preformed $[NbSCl_3(MeCN)_2]$. The structures of the Me-substituted complexes reveal distorted octahedral monomers with the neutral ligands *trans* to S/Cl. Solution ^{1}H and ^{77}Se{^{1}H} NMR data showed that the neutral ligands are partially dissociated and undergoing fast exchange at ambient temperatures in CH_2Cl_2 solution, consistent with weak Lewis acidity for $NbSCl_3$. The complexes containing ^{n}Bu-substituted ligands have been used as single source precursors for low pressure chemical vapour deposition (CVD) of 3R-NbS_2 thin films. 2H-$NbSe_2$ thin films were also obtained *via* low pressure CVD using $[NbSe_2Cl_3(Se^nBu_2)]$. The thin films were characterised by grazing incidence and in-plane XRD, pole figure analysis, scanning electron microscopy and energy dispersive X-ray analysis.

Received 25th May 2017,
Accepted 26th June 2017

DOI: 10.1039/c7dt01911d

rsc.li/dalton

Introduction

Layered early transition metal dichalcogenides ME_2 (M = Nb, Ta, V, W *etc.*, E = S, Se or Te), inorganic analogues of graphite or graphene, are highly stable, and their properties can be tuned by varying the metal and the chalcogen.[1] Applications of these materials in areas such as optoelectronics, spintronics, sensors, electrocatalysis and magnetic materials are being actively developed.[1–3] Production of the materials as thin films maximises the anisotropy of their magnetic or electronic properties and thus methods to deposit 2D layers are of great current interest. Chemical vapour deposition (CVD) is a low cost versatile method to deposit such films using either dual or single source precursors.[4–6] Single source precursors potentially offer better control of deposit stoichiometry, cost-effective use of reagents, and in some cases the ability to selectively deposit the ME_2 onto nano-patterned substrates. Reagents for CVD of NbS_2 or $NbSe_2$ are rare, but include niobium thiolate complexes for the former[7] and a dual source approach using $NbCl_5$-Se^{t}Bu$_2$ for the latter.[6] We recently reported the deposition of thin films of NbS_2 and $NbSe_2$ as the 3R-polytype (R3mh) using $[NbCl_5(S^nBu_2)]$ and $[NbCl_5(Se^nBu_2)]$, respectively, as single source low pressure chemical vapour deposition (LPCVD) precursors.[8] The properties of the potential precursors are key to successful applications in this area, requiring appropriate volatility and clean deposition at accessible temperatures (a β-hydride decomposition route for the neutral ligand is often helpful). Our previous studies showed that Nb(III) dimers such as $[Nb_2Cl_4(E^nBu_2)_2(\mu\text{-}Cl)_2(\mu\text{-}E^nBu_2)]$ did not vaporise under LPCVD conditions, probably due to their high molecular weights,[9] whilst the Nb(IV) complexes such $[NbCl_4(Se^nBu_2)_2]$, $[NbCl_4\{^nBuSe(CH_2)_3Se^nBu\}]$ and $[NbCl_4\{^i$PrSCH$_2$CH$_2$S^{i}Pr$\}]$, lost the chalogenoether on heating *in vacuo*, leaving a residue of the (strongly polymerised) $NbCl_4$.[10]

Here we report on the synthesis and properties of chalcogenoether complexes of niobium chalcogenide trichlorides

Chemistry, University of Southampton, Southampton SO17 1BJ, UK.
E-mail: G.Reid@soton.ac.uk

†Electronic supplementary information (ESI) available: Crystallographic parameters (Table S1), XRD data (Fig. S1) and SEM images (Fig. S2) for the NbS_2 film obtained from $[NbSCl_3\{^nBuS(CH_2)_3S^nBu\}]$ and XRD data from a $NbSe_2$ film obtained by using less $[NbSe_2Cl_3(Se^nBu_2)]$ precursor (~50 mg). Cif files for the four crystallographically characterised precursor complexes. CCDC 1542831–1542834. For ESI and crystallographic data in CIF or other electronic format see DOI: 10.1039/c7dt01911d

$NbECl_3$ (E = S or Se) and attempts to use them as LPCVD reagents. Chalcogenohalides are known for many of the transition elements,[11] although their coordination chemistry has been much less explored than those of the corresponding halides or oxide halides.[12] Complexes of $NbSX_3$ with Lewis bases include $[NbSCl_4]^-$,[13] $[NbSCl_3(Ph_3PS)]$,[14] and $[NbSX_3(Ph_3PO)_2]$ (X = Cl, Br),[15] $[NbSCl_3(SEt_2)]$,[15] and $[NbSX_3(MeCN)_2]$,[15,16] However, in other systems rearrangements occur to form compounds with dichalcogenide bridges, including the structurally characterised $[Nb_2Cl_4(Se_2)_2(L)_4]$ (L = SMe_2 or tetrahydrothiophene (tht)) and $[Nb_2S_3X_4(tht)_4]$.[17,18]

Results and discussion

Complex synthesis and properties

We obtained crude $NbSCl_3$ as a dark green solid by reaction of $NbCl_5$ with $S(SiMe_3)_2$ in CH_2Cl_2 in an ice-bath, and this solid was used to test the parent compound as an LPCVD reagent (see below). As pointed out by others,[19] the colour of $NbSCl_3$ is variously described as golden-yellow to green or black in the literature, and it was suggested that the darker coloured samples contain $Nb_2S_3Cl_4$ impurities. The ν(Nb=S) vibration at 550 cm^{-1} agrees with the literature value.[20]

The thio- and seleno-ether complexes of $NbSCl_3$ were obtained in good yield either by reaction of $NbCl_5$ with the ligand and $S(SiMe_3)_2$ in CH_2Cl_2 in an ice-bath, or by reaction of $[NbSCl_3(MeCN)_2]$ with the ligand in CH_2Cl_2 at ambient temperatures. $[NbSCl_3(MeCN)_2]$ was made by the literature method, involving reaction of $NbCl_5$ with $S(SiMe_3)_2$ in MeCN solution,[16] or by dissolving the crude $NbSCl_3$ in MeCN, filtering to remove any insoluble material, and evaporating the filtrate to dryness. The products of the two methods are spectroscopically identical, and the data agree well with the literature.[15,16]

$[NbSeCl_3(MeCN)_2]$ was obtained from $NbCl_5$ and $Se(SiMe_3)_2$ in MeCN as a brown solid. The IR spectroscopic properties, ν(MeCN) = 2310, 2281, ν(Nb=Se) = 397, ν(Nb–Cl) = 377, 344 cm^{-1}, are as expected, although our assignment of Nb=Se and Nb–Cl vibrations is tentative as they occur at similar frequencies. The ^{93}Nb NMR chemical shift, δ = 923, is at significantly higher frequency than in the thiochloride analogue, reflecting the effect of the selenium coordination.

The reaction of $NbCl_5$ with SMe_2 and $S(SiMe_3)_2$ in CH_2Cl_2 cooled to ~0 °C produced a yellow–green solid of stoichiometry $[NbSCl_3(SMe_2)]$, whilst use of S^nBu_2 gave a dark oil $[NbSCl_3(S^nBu_2)]$. The IR spectrum of $[NbSCl_3(SMe_2)]$ shows a strong vibration at 530 cm^{-1}, assigned as a terminal ν(Nb=S), with ν(Nb–Cl) vibrations at 369, 356, 322 cm^{-1}. In chlorocarbon solution it shows a single δ(Me) resonance in the ^{1}H NMR spectrum, shifted to high frequency from SMe_2, and, more interestingly, a ^{93}Nb NMR resonance[21] at δ = 651. The resonances of niobium thiochloride complexes are found to high frequency of those of $NbCl_5$.[22,23] (Note that the chemical shifts in ref. 22 are reported using the old high frequency negative convention.) The spectroscopic data on $[NbECl_3(S^nBu_2)]$ were similar, suggesting an analogous structure. The X-ray structure of $[NbSCl_3(SMe_2)]$ showed it to be a dimer, $[Nb_2S_2Cl_4(\mu\text{-}Cl)_2(SMe_2)_2]$ (Fig. 1). The bond lengths are unexceptional, with the exception that those associated with the bridging Cl ligands lying *trans* to Nb–S are highly asymmetric. Notably the two SMe_2 ligands are *syn*-disposed, rather than the much more common *anti* arrangement found in many centrosymmetric d-block dimers.

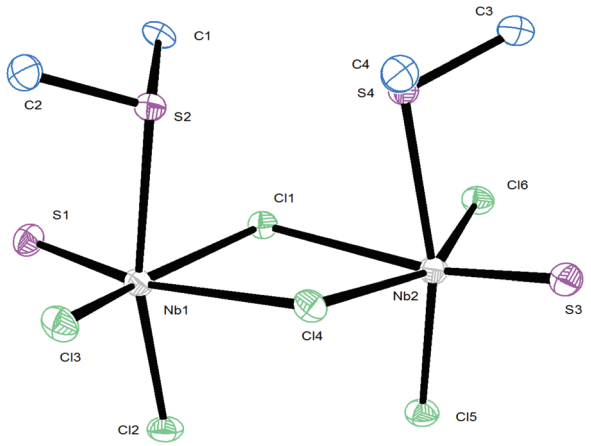

Fig. 1 The structure of $[Nb_2S_2Cl_6(SMe_2)_2]$ showing the atom numbering scheme and with ellipsoids drawn at the 50% probability level. Hydrogen atoms are omitted for clarity. Selected bond lengths (Å): Nb1–S1 = 2.127(2), Nb1–S2 = 2.660(2), Nb1–Cl1 = 2.420(2), Nb1–Cl2 = 2.324(2), Nb1–Cl3 = 2.305(2), Nb1–Cl4 = 2.921(2), Nb2–S3 = 2.123(2), Nb2–S4 = 2.655(2), Nb2–Cl1 = 2.939(2), Nb2–Cl4 = 2.405(2), Nb2–Cl5 = 2.326(2), Nb2–Cl6 = 2.323(2).

The MeCN ligands in $[NbSCl_3(MeCN)_2]$ were cleanly substituted on reaction with an excess (three equivalents) of $MeSCH_2CH_2SMe$, $MeS(CH_2)_3SMe$, $^iPrSCH_2CH_2S^iPr$ or $MeSe(CH_2)_3SeMe$ in CH_2Cl_2 solution at ambient temperatures, to give green $[NbSCl_3(L\text{–}L)]$ (L–L = $MeSCH_2CH_2SMe$, $MeS(CH_2)_3SMe$, $^iPrSCH_2CH_2S^iPr$) or brown $[NbSCl_3\{MeSe(CH_2)_3SeMe\}]$ powdered solids. Using $^nBuS(CH_2)_3S^nBu$ produced $[NbSCl_3\{^nBuS(CH_2)_3S^nBu\}]$ as a green oil. The X-ray crystal structure of $[NbSCl_3\{MeSe(CH_2)_3SeMe\}]$ showed a distorted octahedral geometry, with the in plane terminal S/Cl disordered. The disorder was successfully modelled using split sites for these two atoms and refined at 50 : 50 occupancies; only one form is shown in Fig. 2. The key bond lengths are Nb1–Cl1 = 2.308(7), Nb1–S1 = 2.197(8) Å, whilst the axial Nb1–Cl2 = 2.3686(6) Å, *i.e.* significantly longer.

The structures of two thioether complexes, $[NbSCl_3(MeSCH_2CH_2SMe)]$ and $[NbSCl_3(^iPrSCH_2CH_2S^iPr)]$, were also determined and are shown in Fig. 3 and 4. The X-ray diffraction data were good quality and careful examination did not provide clear evidence for S/Cl disorder in these cases and the d(Nb=S) = 2.10 Å and d(Nb–Cl) = 2.24 Å are nearly identical in the two structures. Notably, the d(Nb–S) distances *trans* to the Nb=S and *trans* to Nb–Cl are different, consistent with a *trans* influence of Nb=S > Nb–Cl. However, as pointed out by others,[14,17,18] it is not possible to rule out some disorder in the

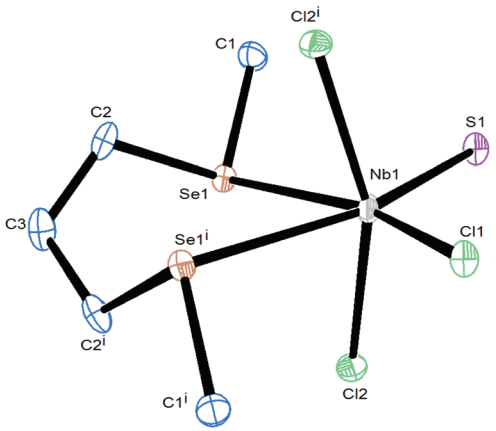

Fig. 2 The structure of $[NbSCl_3\{MeSe(CH_2)_3SeMe\}]$ showing the atom numbering scheme and with ellipsoids drawn at the 50% probability level. Hydrogen atoms are omitted for clarity. Note that S1 and Cl1 are disordered, and only one molecule is shown here. Selected bond lengths (Å) and angles (°): Nb1–Cl1 = 2.308(7), Nb1–Cl2 = 2.3686(6), Nb1–S1 = 2.197(8), Nb1–Se1 = 2.8799(4); Cl1–Nb1–Cl2 = 96.67(15), Cl1–Nb1–$Cl2^i$ = 95.98(15), Cl1–Nb1–S1 = 105.73(5), Cl1–Nb1–$Se1^i$ = 85.29(6), S1–Nb1–Se^1 = 89.90(8), S1–Nb1–Cl2 = 100.1(2), S1–Nb1–$Cl2^i$ = 94.0(2), Cl2–Nb1–Se1 = 79.07(2), Cl2–Nb1–$Se1^i$ = 83.86(2), Se1–Nb1–$Se1^i$ = 79.274(13). Symmetry operation: i = –*x*, –*y* + 3/2, *z*.

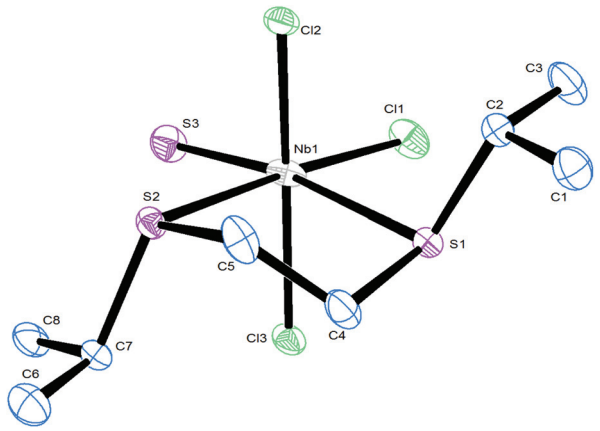

Fig. 4 The structure of $[NbSCl_3(^iPrSCH_2CH_2S^iPr)]$ showing the atom numbering scheme and with ellipsoids drawn at the 50% probability level. Hydrogen atoms are omitted for clarity. Selected bond lengths (Å) and angles (°): Nb1–Cl1 = 2.2475(7), Nb1–Cl2 = 2.3588(6), Nb1–Cl3 = 2.3623(6), Nb1–S1 = 2.7813(6), Nb1–S2 = 2.7464(6), Nb1–S3 = 2.2105(7); Cl1–Nb1–Cl2 = 97.78(2), Cl1–Nb1–Cl3 = 97.49(3), Cl1–Nb1–S1 = 86.78(2), Cl1–Nb1–S3 = 103.84(3), Cl2–Nb1–S1 = 84.58(2), Cl2–Nb1–S2 = 76.69(2), Cl2–Nb1–S3 = 98.20(2), Cl3–Nb1–S1 = 76.73(2), Cl3–Nb1–S2 = 83.48(2), Cl3–Nb1–S3 = 97.13(3), S1–Nb1–S2 = 78.56(2), S2–Nb1–S3 = 91.14(2).

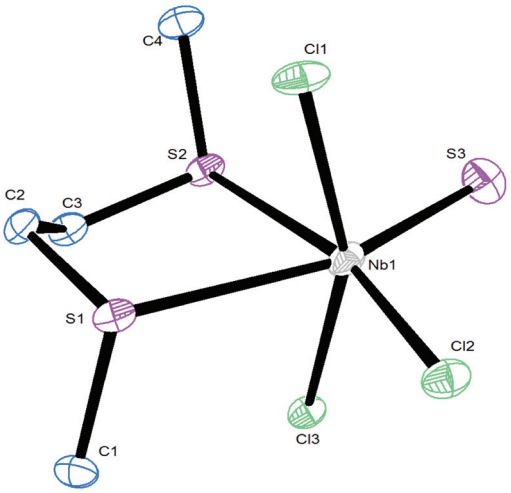

Fig. 3 The structure of $[NbSCl_3(MeSCH_2CH_2SMe)]$ showing the atom numbering scheme and with ellipsoids drawn at the 50% probability level. Hydrogen atoms are omitted for clarity. Selected bond lengths (Å) and angles (°): Nb1–Cl1 = 2.354(1), Nb1–Cl2 = 2.242(1), Nb1–Cl3 = 2.362(1), Nb1–S1 = 2.739(1), Nb1–S2 = 2.717(1), Nb1–S3 = 2.210(1); Cl1–Nb1–Cl2 = 97.52(4), Cl1–Nb1–S1 = 77.05(4), Cl1–Nb1–S2 = 83.36(3), Cl1–Nb1–S3 = 97.13(4), Cl2–Nb1–S1 = 90.37(4), Cl2–Nb1–S3 = 106.56(4), Cl3–Nb1–S2 = 76.78(3), Cl3–Nb1–S3 = 97.00(4), S1–Nb1–S2 = 78.18(3), S2–Nb1–S3 = 85.33(4).

thiochloride systems due to the very similar scattering power of S and Cl atoms. We note in passing that all three structures contain the dichalcogenoether in the *DL* form.

The IR spectra of the five complexes exhibit ν(Nb=S) ~ 525 cm^{-1} and two ν(Nb–Cl) stretches in the range 350–320 cm^{-1}, sometimes with a shoulder on the higher energy vibration, indicating the same molecular geometry. As expected, they are diamagnetic, confirming the presence of d^0 Nb(v). The ^{93}Nb NMR spectra each exhibit a broad resonance in the region δ = +500 to +550, significantly to high frequency of $NbOCl_3$ or $NbCl_5$–thioether complexes.[10,23] The ^{1}H NMR spectrum of $[NbSCl_3(MeSCH_2CH_2SMe)]$ in CD_2Cl_2 at 295 K shows two very broad resonances assignable to δ(MeS) and two $\delta(CH_2)$ resonances, which upon cooling the solution resolve into resonances due to free dithioether[24] and coordinated dithioether, and at 183 K some further splitting is evident, probably due to slowing of pyramidal inversion at the sulfur centres. The data are consistent with some dissociation of the dithioether in solution, and fast exchange between coordinated and 'free' dithioether at ambient temperature. This is further evidence for the weaker Lewis acidity of $NbSCl_3$ compared to $NbOCl_3$ or $NbCl_5$. The ^{1}H NMR spectra of the other four complexes also have broad resonances at ambient temperatures, and show similar changes on cooling the samples. The complex $[NbSCl_3(MeSeCH_2CH_2CH_2SeMe)]$ does not exhibit a $^{77}Se\{^1H\}$ NMR resonance at 295 K, but on cooling to 223 K, resonances due to the 'free' diselenoether (δ = 68),[25] and coordinated diselenoether (δ = 163, 70) appear. The singlet at 70 ppm seems anomalous, but is reproducible and may reflect the 'free' Se donor of a κ^1-coordinated diselenoether, although it is possible this arises due to the Se donor atom *trans* to the terminal S.

Attempts to prepare dithio- or diseleno-ether complexes from $[NbSeCl_3(MeCN)_2]$, even using excess chalcogenoethers or long reaction times, were unsuccessful. However, the reaction of $NbCl_5$ with Se^nBu_2 in CH_2Cl_2, followed by treatment with $(Me_3Si)_2Se$, gave a black solid which, on the basis of

microanalysis and IR and ^{1}H NMR spectroscopic analysis, was tentatively identified as $[NbSe_2Cl_3(Se^nBu_2)]$. The structure of this material is unknown, but it may be dimeric like $[Nb_2Cl_4(Se_2)_2(SMe_2)_2]$ and contain $[Se–Se]^{2-}$ groups.[17]

Application for LPCVD of NbE_2 thin films

Although the gas phase structure of $[NbSCl_3]$ has been determined,[19] indicating some volatility, attempts to use this as a precursor for deposition of NbS_2 in the temperature range 400–750 °C were unsuccessful. However, the complexes, $[NbSCl_3(S^nBu_2)]$, $[NbSCl_3\{^nBuS(CH_2)_3S^nBu\}]$ and $[NbSe_2Cl_3(Se^nBu_2)]$, were likely candidates for use as single source CVD precursors for the low pressure CVD of NbS_2 and $NbSe_2$ thin films, owing to their volatility and the presence of readily eliminated ^{n}Bu groups. Thermogravimetric analyses were undertaken for these complexes (ESI Fig. S4–S6†), and while the mass loss observed does not correspond with the residue being simply NbS_2 or $NbSe_2$, this is unsurprising given the different experimental conditions used for TGA (progressive heating under a flowing argon atmosphere) compared to the vapour transport process involved in the low pressure CVD experiments. However, the TGA experiments do indicate the temperature at which mass loss begins, providing an indication of the low temperature threshold. Low pressure CVD experiments were therefore performed at a pressure of *ca.* 0.05 mmHg using a range of temperatures around 600–750 °C. No significant deposition was observed at lower temperatures.

Black reflective films were obtained from $[NbSCl_3(S^nBu_2)]$ at 700 °C, and grazing incidence XRD showed patterns consistent with NbS_2 in space group *R*3*mh* (3R-type NbS_2) (Fig. 5). These films appear to be air and moisture stable, and lattice parameters determined by Rietveld refinement of the grazing incidence XRD pattern are: a = 3.317(6) and c = 17.79(4) Å (R_{wp} = 6.61%, R_p = 4.46%). These are close to literature values for bulk NbS_2 (a = 3.3303(3), c = 17.918(2) Å).[26] The grazing incident and in-plane XRD patterns shows considerable variations in the intensities of reflections relative to the bulk pattern. The

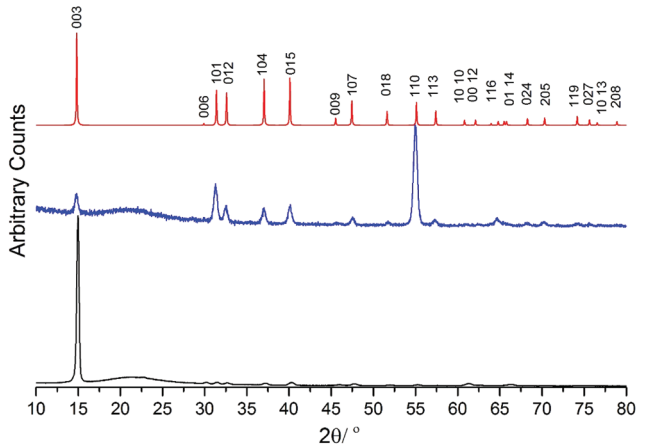

Fig. 5 In plane XRD (blue), grazing incidence (incidence angle = 1°) XRD (black) from the NbS_2 thin film deposited by LPCVD using $[NbSCl_3(S^nBu_2)]$ at 700 °C; simulated XRD pattern from bulk NbS_2 (red).[26] The broad feature at 2θ ~22° is from the SiO_2 substrate.

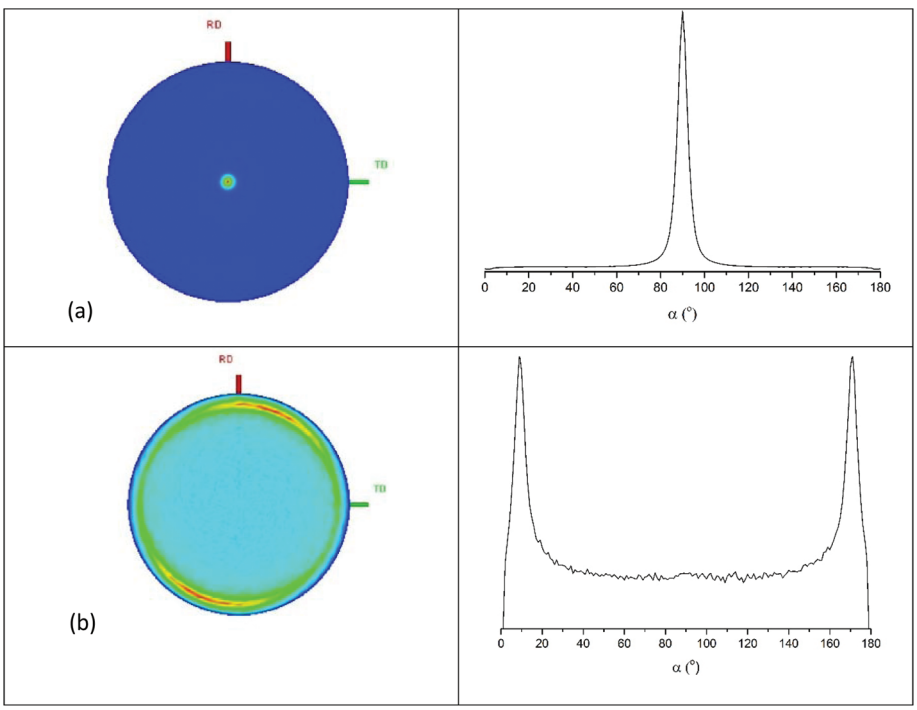

Fig. 6 Pole figures with cut line integral graphs for the 0 0 3 (2θ = 14.97°) (a) and 1 0 1 (2θ = 31.47°) (b) reflections of a film of NbS_2 deposited on a SiO_2 substrate.

003 reflection is the strongest in the grazing incidence XRD pattern, and 101, 012 and 110 reflections are highest in the in-plane XRD pattern, suggesting <00l> preferred orientation.

Pole figure measurements were undertaken on a NbS_2 film obtained from the $[NbSCl_3(S^nBu_2)]$ precursor to establish the film texture. Using 2θ = 14.97°, corresponding to the 0 0 3 reflection, a single, sharp peak (FWHM ~ 5°) was observed at the centre of the figure with α = 90° (Fig. 6a). The figure taken with 2θ = 31.47°, corresponding to the 1 0 1, exhibits a ring with α = 9° (Fig. 6b). These results confirmed the <00l> preferred orientation in which the *ab* planes of the crystallites are parallel with the substrate.

Scanning electron microscopy (SEM) images reveal that the NbS_2 films have a uniform morphology formed of microcrystalline platelets mainly lying flat on the substrate (Fig. 7), consistent with the orientation inferred from the XRD data. EDX data measured at an accelerating voltage of 15 keV show significant Si and O peaks in addition to peaks due to Nb and S, indicating that the films are thin. EDX data also shows there is no evidence for any residual Cl in the films (Cl K_α = 2.621 keV). Accurate quantification of the Nb : S ratio by EDX is difficult due to the Nb L_α and S K_α peaks overlapping.

Films obtained from low pressure CVD using $[NbSCl_3\{^nBuS(CH_2)_3S^nBu\}]$ at 700 °C also present diffraction patterns consistent with *R3mh* (3R-type NbS_2) (Fig. S1†), with lattice parameters a = 3.29(2) and c = 17.8(2) Å (R_{wp} = 5.54%, R_p = 3.47%). SEM images of these films are presented in the ESI (Fig. S2†).

Low pressure CVD experiments were also performed using $[NbSe_2Cl_3(Se^nBu_2)]$ at temperatures between 600 and 700 °C (0.05 mmHg). Films obtained at 650 °C present diffraction patterns consistent with *P*6$_3$/*mmc* (2H-type $NbSe_2$) (Fig. 8). Previously we obtained 3R-$NbSe_2$ from $[NbCl_5(Se^nBu_2)]$.[8] but Parkin and co-workers have reported 2H-$NbSe_2$ by dual source APCVD from $NbCl_5$ and Se^tBu_2.[6] The 002 101 and 110 reflections are the three most intense in both grazing incidence and in-plane XRD patterns, indicating that preferred orientation is not significant in this case. However, using a reduced amount of precursor produces thinner films with evidence of preferred orientation (Fig. S3†). Lattice parameters determined by Rietveld refinement of the grazing incidence XRD pattern are: a = 3.434(7) and c = 12.53(3) Å (R_{wp} = 2.48%, R_p = 1.87%), comparing to the literature values for bulk $NbSe_2$ of a = 3.4446(2), c = 12.5444(7) Å.[27] The $NbSe_2$ films appear to be air and moisture stable. The precursor was also tested in LPCVD at 600 °C however, there is no deposition observed. Scanning electron microscopy (SEM) of the same $NbSe_2$ film shows a polycrystalline film formed of hexagonal platelets mostly oriented with the *c* axis parallel to the substrate (Fig. 9), although the absence of significant preferred orientation from the XRD data suggests it is likely that there are different crystal orientations within the film. Energy dispersive X-ray spectroscopy (EDX) gives the ratio of Nb : Se in the films of 35.8% : 64.2%, with no detectable Cl contamination.

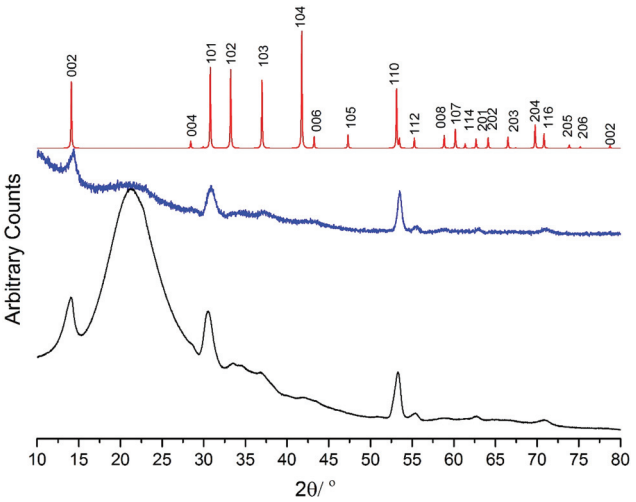

Fig. 8 In plane XRD (blue), grazing incidence (incidence angle = 1°) XRD (black) from the $NbSe_2$ thin film deposited by LPCVD using $[NbSe_2Cl_3(Se^nBu_2)]$ at 650 °C; simulated XRD pattern from bulk $NbSe_2$ (red).[27] The broad feature at 2θ ~22° is from the SiO_2 substrate.

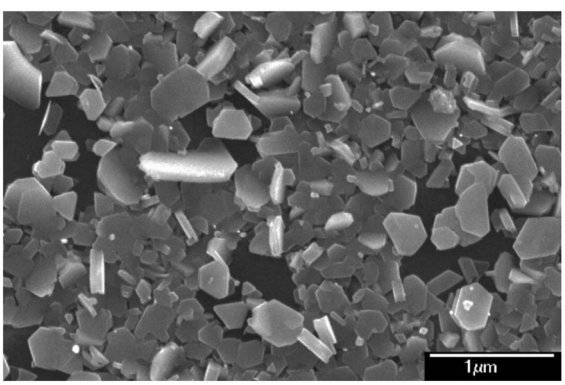

Fig. 7 SEM image of a polycrystalline NbS_2 film deposited by LPCVD from $[NbSCl_3(S^nBu_2)]$ at 700 °C.

Conclusions

A series of thioether and selenoether complexes derived from $NbSCl_3$ is reported. $NbSCl_3$ has been shown to be a weaker Lewis acid than $NbCl_5$. Selected complexes containing ^{n}Bu substituents have been used as single source precursors to produce 3R-NbS_2 thin films *via* low pressure CVD, with preferred <00l> orientation. In contrast, $NbSeCl_3$ does not form similar complexes, however treatment of $[NbCl_5(Se^nBu_2)]$ with $Se(SiMe_3)_2$ forms the complex $[NbSe_2Cl_3(Se^nBu_2)]$ which has been used as a single source precursor for low pressure CVD of 2H-$NbSe_2$ thin films.

Experimental

Syntheses were performed by using standard Schlenk and glove-box techniques under a dry N_2 atmosphere. $NbCl_5$ and

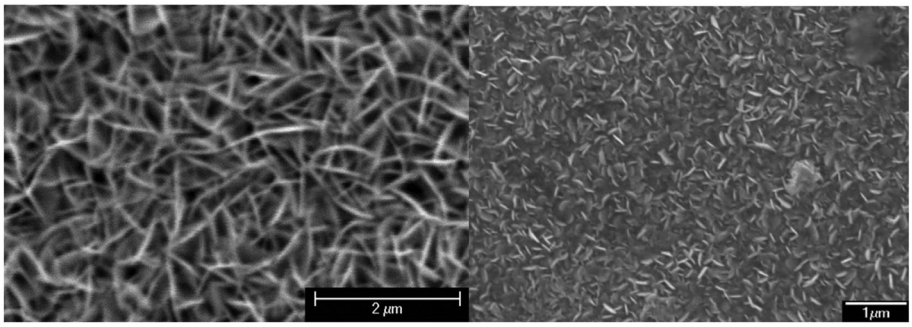

Fig. 9 SEM images of the $NbSe_2$ film deposited from $[NbSe_2Cl_3(Se^nBu_2)]$ at 650 °C.

$S(SiMe_3)_2$ were obtained from Sigma-Aldrich and $Se(SiMe_3)_2$ from Fluorochem and stored in the glovebox in ampoules under N_2. Solvents were dried by distillation from CaH_2 (CH_2Cl_2, MeCN) or Na/benzophenone ketyl (*n*-hexane). Dichalcogenoethers, $RE(CH_2)_nER$ (E = S, Se; n = 2, 3; R = Me, ^{i}Pr, ^{n}Bu), were prepared *via* literature methods.[24,25]

Physical measurements

Infrared spectra were recorded on a PerkinElmer Spectrum 100 spectrometer in the range 4000–200 cm^{-1}, and samples prepared as Nujol mulls between two CsI plates. ^{1}H NMR spectra were recorded using a Bruker AV II 400 spectrometer and referenced to the residual protio-resonance of the solvent. Multinuclear (^{77}Se, ^{93}Nb) NMR spectra were recorded from CD_2Cl_2, $CDCl_3$ or CD_3CN solutions using a Bruker AV II 400 spectrometer and referenced to neat external $SeMe_2$ and $[Et_4N][NbCl_6]$ in MeCN (δ = 0), respectively. Microanalyses on new compounds were undertaken by London Metropolitan University. Thermogravimetric analysis (TGA) data for $[NbSCl_3(S^nBu_2)]$ (ESI Fig. S4†), $[NbSCl_5(^nBuSCH_2CH_2CH_2S^nBu)]$ (ESI Fig. S5†) and $[NbSe_2Cl_3(Se^nBu_2)]$ (ESI Fig. 6†) were collected *via* a Netzsch TG209 F1 Libra analyser under a flow of argon at 65 mL min^{-1}, contained within a dry, nitrogen purged glovebox. The temperature was increased at a rate of 10 °C min^{-1}. Samples were loaded in Al sample pans.

X-ray experimental

Data collections used a Rigaku AFC12 goniometer equipped with an enhanced sensitivity (HG) Saturn724+ detector mounted at the window of an FR-E+ SuperBright molybdenum (λ = 0.71073) rotating anode generator with VHF Varimax optics (70 micron focus) with the crystal held at 100 K (N_2 cryostream). Crystallographic parameters are in the ESI (Table S1†). Structure solution and refinement were performed using SHELX(S/L)97, SHELX-2014/7 and were mostly straightforward, except for the Cl and terminal S atoms of the $[NbSCl_3\{MeSe(CH_2)_3SeMe\}]$ which were disordered and therefore refined with split occupancies giving a 50 : 50 ratio.[28,29] H atoms were added and refined with a riding model.

Complex/precursor preparations. $NbSCl_3$: $NbCl_5$ (405 mg, 1.5 mmol) was suspended in CH_2Cl_2 (20 mL) in an ice bath (0 °C). A solution of $(Me_3Si)_2S$ (260 mg, 1.5 mmol) in CH_2Cl_2 (6 mL) was added with stirring. The solution changed from orange to black immediately and was stirred for 30 min at room temperature. The solvent was removed *in vacuo*, leaving a dark green powder. Yield: 295 mg, 83%. IR (Nujol, cm^{-1}): 550s (Nb═S).

$[NbSCl_3(MeCN)_2]$: Method 1: The complex was prepared by a modified literature method.[16] $NbCl_5$ (405 mg, 1.5 mmol) was dissolved in MeCN (30 mL) and cooled in an ice bath. A solution of $(Me_3Si)_2S$ (260 mg, 1.5 mmol) in MeCN (20 mL) was added. The reaction mixture was then removed from the ice bath and the colour changed from yellow to green over a few minutes. The solution was stirred for 1 h giving a green solution. The solvent was then removed *in vacuo* leaving a yellow–green solid. Yield: 337 mg, 72%. Required for $C_4H_6N_2Cl_3NbS$ (313.33): C, 15.33; H, 1.93; N, 8.94. Found: C, 15.26; H, 1.96; N, 8.82%. IR (Nujol, cm^{-1}): 2316, 2287s (MeCN), 530s (Nb═S), 355sh, 343s, 319s (Nb–Cl). ^{1}H NMR (CD_2Cl_2, 295 K): δ = 1.97 (s, MeCN). ^{93}Nb NMR (CD_3CN, 295 K): δ = 414.

Method 2: $NbSCl_3$ (83 mg, 0.35 mmol) was dissolved in MeCN (20 mL) with stirred for 30 min and giving a dark green solution. The solution was filtered and the filtrate taken to dryness *in vacuo*. Green powder. Yield: 100 mg, 90%. The product was spectroscopically identical to that of $[NbSCl_3(MeCN)_2]$ produced by Method 1.

$[NbSCl_3(SMe_2)]$: $NbCl_5$ (135 mg, 0.5 mmol) was suspended in CH_2Cl_2 (10 mL). SMe_2 (1 mL) was added with stirring for 30 min, giving a dark brown solution. The solution was then cooled in an ice bath (0 °C) and a solution of $S(SiMe_3)_2$ (90 mg, 0.5 mmol) in CH_2Cl_2 (*ca.* 1 mL) was added slowly with stirring for 30 min. The solution was removed from ice bath and stirred for another 5 min and then the volatiles were removed *in vacuo*, leaving a light yellow green solid. Yield: 55 mg, 38%. Required for $C_2H_6Cl_3NbS_2$ (293.46): C, 9.19; H, 2.06. Found: C, 9.29; H, 2.37%. IR (Nujol, cm^{-1}): 530 (Nb═S), 369, 356, 322 (Nb–Cl). ^{1}H NMR ($CDCl_3$, 295 K): δ = 2.32 (s, SMe_2). ^{93}Nb NMR (CD_2Cl_2, 295 K): δ = 651. Yellow–green crystals grew by allowing CH_2Cl_2 solution to evaporate slowly under a nitrogen atmosphere.

$[NbSCl_3(S^nBu_2)]$: $NbCl_5$ (270 mg, 1.0 mmol) was suspended in CH_2Cl_2 (10 mL) and a solution of S^nBu_2 (147 mg, 1.0 mmol) in CH_2Cl_2 (3 mL) was added with stirring. After 15 min an orange solution formed. A solution of $S(SiMe_3)_2$ (179 mg,

1.0 mmol) and CH_2Cl_2 (3 mL) was added with stirring. The colour changed to dark green after stirring for 30 min. The solution was taken to dryness *in vacuo*, leaving a sticky oil which was washed with *n*-hexane (5 mL), before drying *in vacuo*. Thick dark oil. Yield: 331 mg, 88%. Required for $C_8H_{18}Cl_3NbS_2$ (377.62): C, 25.44; H, 4.80. Found: C, 25.58; H, 4.88%. IR (Nujol, cm^{-1}): 554 (Nb═S), 387, 374, 359sh (Nb–Cl). ^1H NMR ($CDCl_3$, 295 K): δ = 0.97 (t, [6H], Me), 1.48 (m, [4H], CH_2Me), 1.74 (m, [4H], $SCH_2CH_2CH_2$), 2.94 (t, [4H], SCH_2). ^{93}Nb NMR (CD_2Cl_2, 295 K): δ = 654.

[$NbSCl_3(Se^nBu_2)$]: $NbCl_5$ (270 mg, 1.0 mmol) was suspended in CH_2Cl_2 (10 mL) and a solution of Se^nBu_2 (193 mg, 1.0 mmol) in CH_2Cl_2 (3 mL) was added with stirring, giving a red solution, which was stirred for 1 h. $S(SiMe_3)_2$ (0.21 mL, 1.0 mmol) was then added. The solution turned dark green, and after stirring for 30 min the solvent was removed *in vacuo* to leave a sticky oil. After washing with hexane (5 mL), the oil was dried *in vacuo*. Sticky black oil. Yield: 200 mg, 47%. Required for $C_8H_{18}Cl_3NbSSe$ (424.52): C, 22.63; H, 4.27. Found: C, 22.52; H, 4.29%. IR (Nujol, cm^{-1}): 530 (Nb═S), 380, 366, 355sh (Nb–Cl). ^1H NMR ($CDCl_3$, 295 K): δ = 0.93 (t, [6H], Me), 1.42 (m, [4H], CH_2Me), 1.66 (m, [4H], $SeCH_2CH_2$), 2.61 (br, [4H], $SeCH_2$). ^{77}Se (CD_2Cl_2, 295 K): no resonance. ^{93}Nb NMR (CD_2Cl_2, 295 K): δ = 694.

[$NbSCl_3(MeSCH_2CH_2SMe)$]: [$NbSCl_3(MeCN)_2$] (94 mg, 0.3 mmol) was dissolved in CH_2Cl_2 (10 mL) at room temperature. A solution of $MeSCH_2CH_2SMe$ (110 mg, 0.9 mmol) and CH_2Cl_2 (1 mL) was added and the solution stirred for 30 min. Some green-yellow powder formed in the solution. After filtering, the green solution was evaporated to dryness *in vacuo*. *n*-Hexane (10 mL) was added to wash the solid which was separated and dried *in vacuo*. Yield: 67 mg, 63%. Required for $C_4H_{10}Cl_3NbS_3$ (353.58): C, 13.59; H, 2.85. Found: C, 13.64; H, 2.93%. IR (Nujol, cm^{-1}): 526 (Nb═S), 361sh, 349, 319 (Nb–Cl). ^1H NMR (CD_2Cl_2, 295 K): δ = 2.22 (br, [3H], $SMe_{trans\ Cl}$), 2.78 (br, [3H], $SMe_{trans\ S}$) 3.04(s), 3.26(s) ([4H], CH_2); (183 K): 2.06 (s, [6H], Me), 2.63 (s, [4H], CH_2) (both 'free' dithoether), 2.12 (s, [3H]), 2.18 (s, [3H]), 2.76, 2.94 (CH_2) (coord. dithioether) (see text). ^{93}Nb NMR (CD_2Cl_2, 295 K): δ = 507. Green crystals grew by allowing a CH_2Cl_2 solution to evaporate under a dinitrogen atmosphere.

[$NbSCl_3(^iPrSCH_2CH_2S^iPr)$]: Was made similarly and isolated as a green powder. Yield: 76%. Required for $C_8H_{18}Cl_3NbS_3$ (409.69): C, 23.45; H, 4.43. Found: C, 23.27; H, 4.41%. IR (Nujol, cm^{-1}): 527 (Nb═S), 365 (sh), 348, 318 (Nb–Cl). ^1H NMR (CD_2Cl_2, 295 K): δ = 1.32 (br s, [6H], SMe), 1.59 (br s, [6H], SMe), 3.01–3.28 (br, [4H], SCH_2), 3.46 (br, [2H], SCH). ^{93}Nb NMR (CD_2Cl_2, 295 K): δ = 523. Green crystals grew by allowing a CH_2Cl_2 solution to evaporate slowly under a dinitrogen atmosphere.

[$NbSCl_3\{MeS(CH_2)_3SMe\}$]: Was made similarly and isolated as a green solid. Yield: 68% Required for $C_5H_{12}Cl_3NbS_3$ (367.61): C, 16.34; H, 3.29. Found: C, 16.48; H, 3.21%. IR (Nujol, cm^{-1}): 524 (Nb═S), 369 sh, 345, 323 (Nb–Cl). ^1H NMR ($CDCl_3$, 295 K): δ = 2.14 (br, [2H], SCH_2CH_2), 2.45 (vbr, [6H], SMe), 2.96 (vbr, [4H], SCH_2). ^{93}Nb NMR (CD_2Cl_2, 295 K): δ = 530.

[$NbSCl_3\{^nBuS(CH_2)_3S^nBu\}$]: Was made similarly and isolated as a dark green oil after washing with *n*-hexane, decanting off the washings and drying *in vacuo*. Yield: 76%. Required for $C_{11}H_{24}Cl_3NbS_3$ (451.77): C, 29.24; H, 5.35. Found: C, 29.37; H, 5.45%. IR (Nujol, cm^{-1}): 529 (Nb═S), 349, 322 (Nb–Cl). ^{93}Nb NMR (CD_2Cl_2, 295 K): δ = 534.

[$NbSCl_3\{MeSe(CH_2)_3SeMe\}$]: Was made similarly and isolated as a yellow brown powder. Yield: 58%. Required for $C_5H_{12}Cl_3NbSSe_2$ (461.40): C, 13.02; H, 2.62. Found: C, 13.17; H, 2.74%. IR (Nujol, cm^{-1}): 521 (Nb═S), 342, 320 (Nb–Cl). ^1H NMR (CD_2Cl_2, 295 K): δ = 2.25 (br, [8H], SeMe and CH_2CH_2Se), 2.92 (br, [4H], CH_2Se). $^{77}Se\{^1H\}$ NMR (CD_2Cl_2, 295 K): no resonance; (223 K): δ = 163, 70, 68. ^{93}Nb NMR (CD_2Cl_2, 295 K): δ = 547. Yellow crystals grew by allowing a CH_2Cl_2 solution to evaporate under a dinitrogen atmosphere.

[$NbSeCl_3(MeCN)_2$]: $NbCl_5$ (135 mg, 0.5 mmol) was dissolved in MeCN (10 mL). A solution of $Se(SiMe_3)_2$ (113 mg, 0.5 mmol) in MeCN (5 mL) was then added and the reaction mixture was stirred for 30 min. The colour changed to dark brown. The solvent was removed *in vacuo* leaving a brown solid. Yield: 150 mg, 83%. Required for $C_4H_6Cl_3N_2NbSe$ (360.33): C, 13.33; H, 1.68; N, 7.77. Found: C, 13.25; H, 1.65; N, 7.57%. IR (Nujol, cm^{-1}): 2310, 2281 (MeCN), 397 (Nb═Se?), 377, 344 (Nb–Cl). ^{93}Nb NMR (CD_2Cl_2, 295 K): δ = 923.

[$NbSe_2Cl_3(Se^nBu_2)$]: $NbCl_5$ (235 mg, 0.88 mmol) was suspended in CH_2Cl_2 (20 mL). A solution of $^nBu_2Se$ (177 mg, 0.88 mmol) and CH_2Cl_2 (*ca.* 1.5 mL) was added with stirring for 1 hour. The reaction mixture changed colour to dark red and all the $NbCl_5$ dissolved. A solution of $Se(SiMe_3)_2$ (0.22 mL, 0.88 mmol) and CH_2Cl_2 (*ca.* 1.7 mL) was added, causing a colour change from dark red to black. The solution was stirred for 15 min before it was taken to dryness *in vacuo*. The resulting black solid was washed with *n*-hexane (15 mL) and then dried *in vacuo*. Yield: 298 mg, 61%. Required for $C_8H_{18}Cl_3NbSe_3$ (550.37): C, 17.46; H, 3.3. Found: C, 17.59; H, 3.38. IR (Nujol, cm^{-1}): 344, 319, 272 (Nb–Cl). ^1H NMR ($CDCl_3$, 295 K): δ 0.94 (t, [6H], Me), 1.44 (m, [4H], CH_2Me), 1.70 (m, [4H], $SeCH_2CH_2CH_2$), 2.71 (t, [4H], $SeCH_2$).

LPCVD general procedure. The precursor (20–100 mg) was loaded into the end of a silica tube in an N_2 purged glove box. Then the silica substrates (~1 × 8 × 20 mm^3) were loaded in the tube and placed end-to-end. The tube was set in a furnace so that the substrates were in the heated zone and the precursor was *ca.* 2 cm away from the start of the heated zone. The tube was evacuated to 0.5 mmHg, and the furnace was heated to the requisite temperature between 600 and 800 °C. The tube was then moved into the furnace. The position of the sample was maintained until the all the precursor had evaporated. The tube was then cooled to room temperature and the tiles were unloaded at ambient temperature and stored in air.

LPCVD from [$NbSCl_3(S^nBu_2)$], [$NbSCl_3\{^nBuS(CH_2)_3S^nBu\}$] and [$NbSe_2Cl_3(Se^nBu_2)$] resulted in deposition of reflective black films on tiles positioned in the hotter region of the furnace (*i.e.* NbS_2 actual deposition temperature ~670 °C;

$NbSe_2$ actual deposition temperature ~625 °C – measured by profiling the furnace).

Film characterisation. X-Ray diffraction (XRD) patterns were collected in grazing incidence mode (θ_1 = 1°) or in-plane mode (θ_1 = 0.5°, $2\theta_\chi$ scan with the detector scanning in the film plane) using a Rigaku SmartLab diffractometer (Cu-K_α, λ = 1.5418 Å) with parallel X-ray beam and a DTex Ultra 250 1D detector. Phase matching and lattice parameter refinement used the PDXL2 software package[30] and diffraction patterns from ICSD.[31]

Scanning electron microscopy (SEM) was performed on samples of $NbSe_2$ using a Philips XL30 ESEM and with an acceleration voltage of 10 kV or 15 kV, whilst SEM measurements on NbS_2 films used a JEOL JSM6500 and an accelerating voltage of 10 kV.

Energy dispersive X-ray (EDX) data on $NbSe_2$ samples were obtained at accelerating voltage of 10 and 15 kV with a Thermofisher Ultradry NSS 3 (XL30) detector or at an accelerating voltage of 15 kV with an Oxford INCA x-act X-ray detector (JSM6500) for NbS_2 samples.

Acknowledgements

We thank the EPSRC for funding the SmartLab diffractometer (*via* EP/K00509X/1 and EP/K009877/1) and the University of Southampton for a VC Scholarship (to Y.-P. C).

References

1 M. Chhowalla, Z. Liu and H. Zhang, (Eds. - themed issue on metal dichalcogenides) Chem. Soc. Rev., 2015, **44**, 2584.
2 M. Chhowalla, H. S. Shin, G. Eda, L.-J. Li, K. P. Loh and H. Zhang, *Nat. Chem.*, 2013, **5**, 263; J. Liu and X.-W. Liu, *Adv. Mater.*, 2012, **24**, 4097.
3 Q. Xiang, J. Yu and M. Jaroniec, *J. Am. Chem. Soc.*, 2012, **134**, 6575; J. Pu, Y. Yomogida, K.-K. Liu, L.-J. Li, Y. Iwasa and T. Takenobu, *Nano Lett.*, 2012, **12**, 4013; K. Lee, R. Gatensby, N. McEvoy, T. Hallam and G. S. Duesberg, *Adv. Mater.*, 2013, **25**, 6699; Y. Ma, Y. Dsi, M. Guo, C. Niu, Y. Zhu and B. Huang, *ACS Nano*, 2012, **6**, 1695; K. Xu, P. Chen, X. Li, C. Wu, Y. Guo, J. Zhao, X. Wu and Y. Xie, *Angew. Chem., Int. Ed.*, 2013, **52**, 10477; H. Li, G. Lu, Y. Wang, Z. Yin, C. Cong, Q. He, L. Wang, F. Ding, T. Yu and H. Zhang, *Small*, 2013, **9**, 1974; Z. Yan, C. Jiang, T. R. Pope, C. F. Tsang, J. L. Stickney, P. Goli, J. Renteria, T. T. Salguero and A. A. Balandin, *J. Appl. Phys.*, 2013, **114**, 20430.
4 A. C. Jones and M. L. Hitchman, in *Chemical Vapour Deposition: Precursors, Processes and Applications*, ed. A. C. Jones and M. L. Hitchman, The Royal Society of Chemistry, 2009.
5 P. J. McKarns, T. S. Lewkebandara, G. P. A. Yap, L. M. Liable-Sands, A. L. Rheingold and C. H. Winter, *Inorg. Chem.*, 1998, **37**, 418; S. D. Reid, A. L. Hector, W. Levason, G. Reid, B. J. Waller and M. Webster, *Dalton Trans.*, 2007, 4769; S. L. Benjamin, C. H. de Groot, C. Gurnani, A. L. Hector, R. Huang, K. Ignatyev, W. Levason, S. J. Pearce, F. Thomas and G. Reid, *Chem. Mater.*, 2013, **25**, 4719; N. D. Boscher, C. J. Carmalt and I. P. Parkin, *Chem. Vap. Deposition*, 2006, **12**, 54.
6 N. D. Boscher, C. J. Carmalt and I. P. Parkin, *Eur. J. Inorg. Chem.*, 2006, 1255.
7 E. S. Peters, C. J. Carmalt, I. P. Parkin and D. A. Tocher, *Eur. J. Inorg. Chem.*, 2005, 4179; C. J. Carmalt, E. S. Peters, I. P. Parkin, T. D. Manning and A. L. Hector, *Eur. J. Inorg. Chem.*, 2004, 4470.
8 S. L. Benjamin, Y.-P. Chang, C. Gurnani, A. L. Hector, M. Huggon, W. Levason and G. Reid, *Dalton Trans.*, 2014, **43**, 16640.
9 S. L. Benjamin, Y.-P. Chang, M. Huggon, W. Levason and G. Reid, *Polyhedron*, 2015, **99**, 230.
10 Y.-P. Chang, W. Levason, M. E. Light and G. Reid, *Dalton Trans.*, 2016, **45**, 16262.
11 D. A. Rice, *Coord. Chem. Rev.*, 1978, **25**, 199; M. J. Atherton and J. H. Holloway, *Adv. Inorg. Chem. Radiochem.*, 1979, **22**, 171.
12 *Comprehensive Coordination Chemistry II*, ed. T. J. Meyer and J. A. McCleverty, Elsevier, Oxford, 2004, vol. 4 and 5.
13 U. Müller and P. Klingelhöfer, *Z. Anorg. Allg. Chem.*, 1984, **510**, 109.
14 M. G. B. Drew and R. J. Hobson, *Inorg. Chim. Acta*, 1983, **72**, 233.
15 K. Behzadi, A. G. Baghlaf and A. Thomson, *J. Less-Common Met.*, 1987, **128**, 195.
16 V. C. Gibson, A. Shaw and D. N. Williams, *Polyhedron*, 1989, **8**, 549.
17 M. G. B. Drew, D. A. Rice and D. M. Williams, *J. Chem. Soc., Dalton Trans.*, 1984, 1087; M. G. B. Drew, D. A. Rice and D. M. Williams, *Acta Crystallogr.*, 1980, **C40**, 1547.
18 M. G. B. Drew, D. A. Rice and D. M. Williams, *J. Chem. Soc., Dalton Trans.*, 1983, 2251.
19 I. Nowak, E. M. Page, D. A. Rice, A. D. Richardson, R. J. French, K. Hedberg and J. S. Ogden, *Inorg. Chem.*, 2003, **42**, 1296.
20 G. W. A. Fowles, R. J. Hobson, D. A. Rice and K. J. Shanton, *J. Chem. Soc., Chem. Commun.*, 1976, 552.
21 ^{93}Nb, 100%, I = 9/2, Ξ = 24.44, R_c = 2740, $Q = -0.2 \times 10^{-28}$ m^2. J. Emsley, *The Elements*, Oxford, 1989.
22 V. P. Tarasov, S. M. Sinitsyna, V. D. Kopanev, V. G. Khleboradov and Y. A. Buslaev, *Koord. Khim.*, 1980, **6**, 1568.
23 W. Levason, M. Jura, R. Ratnani, G. Reid and M. Webster, *Dalton Trans.*, 2010, **49**, 883.
24 F. R. Hartley, S. G. Murray, W. Levason, H. E. Soutter and C. A. McAuliffe, *Inorg. Chim. Acta*, 1979, **35**, 265.
25 D. J. Gulliver, E. G. Hope, W. Levason, S. G. Murray, D. M. Potter and G. L. Marshall, *J. Chem. Soc., Perkin Trans. 2*, 1984, 429.

26 B. Morosin, *Acta Crystallogr., Sect. B: Struct. Crystallogr. Cryst. Chem.*, 1974, **30**, 551.
27 B. E. Brown and D. J. Beerntsen, *Acta Crystallogr.*, 1965, **18**, 31.
28 G. M. Sheldrick, *Acta Crystallogr., Sect. C: Cryst. Struct. Commun.*, 2015, **71**, 3.
29 *CrysAlis PRO*, Agilent Technologies Ltd., Yarnton, Oxfordshire, England.
30 S. Grazulis, D. Chateigner, R. T. Downs, A. F. Yokochi, M. Quiros, L. Lutterotti, E. Manakova, J. Butkus, P. Moeck and A. Le Bail, *J. Appl. Crystallogr.*, 2009, **42**, 726.
31 ICSD: Inorganic Crystal Structure Database (ICSD), Fachinformationszentrum Karlsruhe (FIZ), accessed via the United Kingdom Chemical Database Service, D. A. Fletcher, R. F. McMeeking and D. J. Parkin, *Chem. Inf. Comput. Sci.*, 1996, **36**, 746.